中山大学 中山眼科中心 ZHONGSHAN OPHTHALMIC CENTER, SUN YAT-SEN UNIVERSITY

全文收录于 Lighthouse Scholar

眼科学报

官网： journal.gzzoc. com



doi: 10.12419/24110202
View this article at: https://dx.doi.org/10.12419/24110202

·综述·

眼底老化相关沉积物的病理、多模态影像及临床意义

蔡金玉 综述，蒋燕梅，陈玲 审校

（重庆医科大学附属第一医院眼科，重大致盲眼病防治重庆市重点实验室，重庆市眼科研究所，重庆 400016）

文章亮点

1. 关键发现

- 通过总结几种重要眼底老化相关沉积物的病理特征和多模态影像学表现，帮助认识和理解其眼底表现、组织病理特点和形成机制，以及在年龄相关性黄斑变性 (age-related macular degeneration, AMD) 发生及进展中的临床意义。

2. 已知与发现

- 眼底老化是 AMD 的关键病理基础，其特征之一是随着年龄增长外层视网膜出现异常物质沉积，即眼底老化相关沉积物的形成。脂质代谢紊乱在这些沉积物的形成机制中扮演着至关重要的角色。

3. 意义与改变

- 本文针对几种眼底老化相关沉积物的病理、多模态影像及临床意义进行综述，关注脂质代谢紊乱在眼底老化及早期 AMD 启动机制中的显著意义，有助于加深和丰富眼底老化相关沉积物的临床病理及影像学认识，为早期 AMD 的干预和治疗找到新的突破口。

[摘　要]　眼底老化是年龄相关性黄斑变性(age-related macular degeneration, AMD)发生和进展的关键因素及病理基础，在组织病理学上主要表现为脉络膜毛细血管萎缩、布鲁赫膜(Bruch's membrane, BrM)增厚以及视网膜色素上皮(retinal pigment epithelium, RPE)异常。BrM增厚可由多种眼底老化沉积物聚集引起，在AMD的病理机制中具有重要作用。其中，基底薄层沉积物(basal laminar deposit, BLamD)代表了RPE基底膜的弥漫性增厚，通常作为一种正常眼底老化改变。而以酯化和未酯化胆固醇等中性脂质为主的RPE基底膜下沉积物，即基底线性沉积物(basal linear deposits, BLinD)和软性玻璃膜疣，均可参与破坏脉络膜与外层视网膜间物质交换稳态，造成外层视网膜缺血、缺氧及氧化应激，是AMD早期重要病理改变。硬性玻璃膜疣主要分布于周边视网膜，多见于正常老化眼底；表皮玻璃膜疣是RPE基底膜局灶性结节状增厚的结果，眼底表现与硬性玻璃膜疣相似，但其主要分布于后极部，数量更多且密度更高。近年来逐渐加深

收稿日期(Received): 2024-11-11; **修订日期(Revised)**: 2024-12-12; **接收日期(Accepted)**: 2024-12-25

通信作者(Corresponding author): 陈玲，Email: ling-ch@163.com

基金项目(Foundation item): 国家自然科学基金面上项目（82171083）。This work was supported by National Natural Science Foundation of China General Program (82171083).

作者贡献声明: 构思设计:蔡金玉, 陈玲; 行政支持: 陈玲; 提供研究材料: 蔡金玉, 陈玲, 蒋燕梅; 数据收集与汇总: 蔡金玉, 蒋燕梅; 数据分析与解读: 蔡金玉, 陈玲; 稿件撰写: 蔡金玉, 陈玲; 稿件最终修订与同意:所有作者。

Contributions: Conception and design: CAI Jinyu, CHEN Ling; Administrative support: CHEN Ling; Provision of study materials: CAI Jinyu, CHEN Ling, JIANG Yanmei; Collection and assembly of data: CAI Jinyu, JIANG Yanmei; Data analysis and interpretation; CAI Jinyu, CHEN Ling; Manuscript writing: CAI Jinyu, CHEN Ling; Final approval of manuscript: All authors

电子全文

了对视网膜下玻璃膜疣样沉积物(subretinal drusenoid deposit, SDD)的认识和研究，其是位于RPE上方的沉积物，在AMD发病机制中亦具有深刻意义。文章就几种眼底老化相关沉积物(包括硬性玻璃膜及表皮玻璃膜疣)的病理特征和多模态影像学表现进行综述，旨在帮助认识和理解这些沉积物的眼底表现、病理特征和形成机制，以及在AMD发生及进展中的临床意义。

[关键词] 眼底老化；年龄相关性黄斑变性；脂质沉积；玻璃膜疣；病理；多模态影像学

[中图分类号] R774.5， R772.5 **[文献标志码]** A

引用本文：蔡金玉, 蒋燕梅, 陈玲. 眼底老化相关沉积物的病理、多模态影像及临床意义[J]. 眼科学报, 2025, 40(2): 155-170. DOI: 10.12419/24110202.

Pathology, multimodal imaging and clinical significance of age-related fundus deposits

CAI Jinyu, JIANG Yanmei, CHEN Ling

(Department of Ophthalmology, Chongqing Key Laboratory for the Prevention and Treatment of Major Blinding Eye Diseases, Chongqing Eye Institute, The First Affiliated Hospital of Chongqing Medical University, Chongqing 400016, China)

Abstract Fundus aging is a key factor and pathological basis for the development and progression of age-related macular degeneration (AMD), which is histopathologically characterized by choroidal capillary atrophy, Bruch's membrane (BrM) thickening, and abnormalities of retinal pigment epithelium (RPE). BrM thickening can be induced by the aggregation of age-related fundus deposits and plays an essential role in the pathogenesis of AMD. Basal laminar deposits (BLamD) represent diffuse thickening of the basement membrane of RPE, usually considered to be a normal fundus aging. Basal linear deposits (BLinD) and soft drusen, mainly composed of neutral lipids such as esterified and unesterified cholesterol, can disrupt the homeostasis of material exchange between the choroid and the outer retina, resulting in ischemia, hypoxia, and oxidative stress in the outer retina, which are important pathological changes in the early AMD. Hard drusen is mainly distributed in the peripheral retina and is very common in aging fundus; Cuticular drusen are resulted from focal nodular thickening of the basement membrane of RPE, with similar appearance as hard drusen, but mainly distributed in the posterior pole and more numerous and denser. Recently, our understanding of subretinal drusenoid deposits (SDD), deposits above the RPE, has been gradually deepened and it also has profound significance in the pathogenesis of AMD. In this review, we presented the pathologic features and multimodal imaging of age-related fundus deposits (including hard drusen and cuticular drusen), aiming to help recognize and understand the manifestations, pathologic features, and formation mechanisms of these deposits, as well as their clinical significance in the development and progression of AMD.

Keywords fundus aging; age-related macular degeneration; lipid deposits; soft drusen; pathology; multimodal imaging

Cite this article as: CAI Jinyu, JIANG Yanmei, CHEN Ling. Pathology, multimodal imaging and clinical significance of age-related fundus deposits[J]. Yan Ke Xue Bao, 2025, 40(2): 155-170. DOI: 10.12419/24110202.

年龄相关性黄斑变性(age-related macular degeneration, AMD)是老年人最主要的致盲眼病之一，其发病机制尚不完全清楚。随着年龄增长而出现的眼底老化是AMD发生及进展的关键因素和病理基础[1]。病理研究表明，与AMD相关的眼底老化主要出现在外层视网膜，包括脉络膜毛细血管萎缩、布鲁赫膜(Bruch's membrane, BrM)增厚以及视网膜色素上皮(retinal pigment epithelium, RPE)异常[2]。软性玻璃膜疣为AMD的早期标志性病变，BrM增厚等眼底老化相关脂质沉积为AMD更早期的亚临床病理改变，在AMD的发生及进展中具有重要意义。随着多模态影像技术的不断发展，结合组织病理学研究，研究者对眼底老化相关沉积物的认识逐渐深入，并对其在AMD发病机制中的重要性亦逐渐明了。本文将简要概述外层视网膜的解剖结构特征，重点介绍眼底老化相关沉积物的病理特征、多模态影像学表现及临床意义，并基于此对未来研究方向提出新的展望。

1 外层视网膜的解剖特征及重要性

组织学上将视网膜分为10层结构，从外到内依次为RPE层、光感受器层、外界膜、外核层、外丛状层、内核层、内丛状层、神经节细胞层、神经纤维层和内界膜[3]。通常以外丛状层-内核层交界为界，将视网膜概括为外五层（图1）和内五层[4]，位于外层视网膜的光感受器-RPE-脉络膜毛细血管复合体是参与视觉形成的关键结构，三者密切配合，共同完成视觉信号转换、营养供给以及代谢处理等功能[3]。光感受器包括负责暗视觉的视杆细胞和负责颜色及细节分辨的视锥细胞，二者数量比约为20:1[5]。RPE由单层极化色素上皮细胞所组成，细胞间有紧密连接，参与构成血-视网膜外屏障，调控外层视网膜与脉络膜之间的物质交换[6-7]。RPE细胞顶端连接光感受器外节(photoreceptor outersegments, OS)，能够吞噬脱落OS并有助于光感受器细胞的维持更新[8]。RPE细胞的基底端连接BrM，病理学上将BrM分为5层结构，包括RPE基底膜、内胶原层、弹力层、外胶原层和脉络膜毛细血管基底膜，BrM为固定支撑RPE和脉络膜毛细血管，以及维持外层视网膜和脉络膜循环间的代谢稳态发挥生理功能[9]。

2 眼底老化相关沉积物

眼底老化在病理学上主要表现为脉络膜毛细血管萎缩、BrM增厚及RPE异常[2]。BrM增厚广义上包括了多种眼底老化相关沉积物的形成，其主要是由于脂质等物质的异常积聚引起[10-11]。一方面，脂质过氧化可引起炎症反应和氧化应激，另一方面，中性脂质会阻碍外层视网膜与脉络膜循环之间的物质交换，引起外层视网膜缺血、缺氧，导致血管内皮生长因子(vascular endothelial growth factor, VEGF)等产生增多，进一步损害RPE和光感受器[12]。眼底老化相关沉积物的形成与RPE异常以及脉络膜毛细血管萎缩均关系密切。RPE细胞的衰老和功能紊乱是产生细胞外沉积物，即AMD特征性病理改变的根源所在，而随着年龄增长出现的脉络膜毛细血管萎缩会导致RPE细胞外沉积物不能及时被脉络膜循环清除而逐渐积聚在BrM[13]。位于RPE和BrM之间的异常沉积被称为RPE下沉积，包括基底薄层沉积物(basal laminar deposit, BLamD)、基底线性沉积物(basal linear deposits, BLinD)和其前体(Pre-BLinD)，以及AMD传统意义上的标志性沉积物——软性玻璃膜疣(图1)。此外，还包括硬性玻璃膜疣、表皮玻璃膜疣，以及沉积于RPE上方的视网膜下玻璃膜疣样沉积物(subretinal drusenoid deposit, SDD)（图1）等。本文将重点介绍上述几类眼底老化相关沉积物的病理特征，多模态影像学表现及其临床意义。

2.1 BLamD

BLamD被认为是RPE细胞质膜与RPE基底膜之间增多的细胞外基质，主要由基底膜蛋白及纤维胶原物质构成，也包含酯化和未酯化胆固醇及C3等补体成分[15-16]。现认为其代表了RPE基底膜的弥漫性增厚，通常作为一种正常眼底老化改变，可见于大部分老年人。BLamD呈弥漫性分布，可于黄斑区和周边部视网膜被观察到，并能反映出RPE细胞的应激状态[17-18]。多种因素均可诱发BLamD，包括吸烟、高脂饮食以及光化学损伤等[19-20]。BLamD也可存在于一些病理条件下，如迟发性视网膜变性和Sorsby眼底营养不良等疾病[21-22]。此外，BLamD在AMD患眼中非常多见，但并非AMD的特异性病变，组织学下表现为RPE与其基底膜间增厚的连续层状沉积[23](图2 B、D、F)。Curcio教授团队根据BLamD的组织学特征将其分为早期BLamD、晚期BLamD和持续性BLamD等[24]。常规的眼底检查无法检测到形成初期的BLamD(图2A)，仅可通过病理学手段或在透射电子显微镜下进行定位和定性，以及实现与BLinD的区

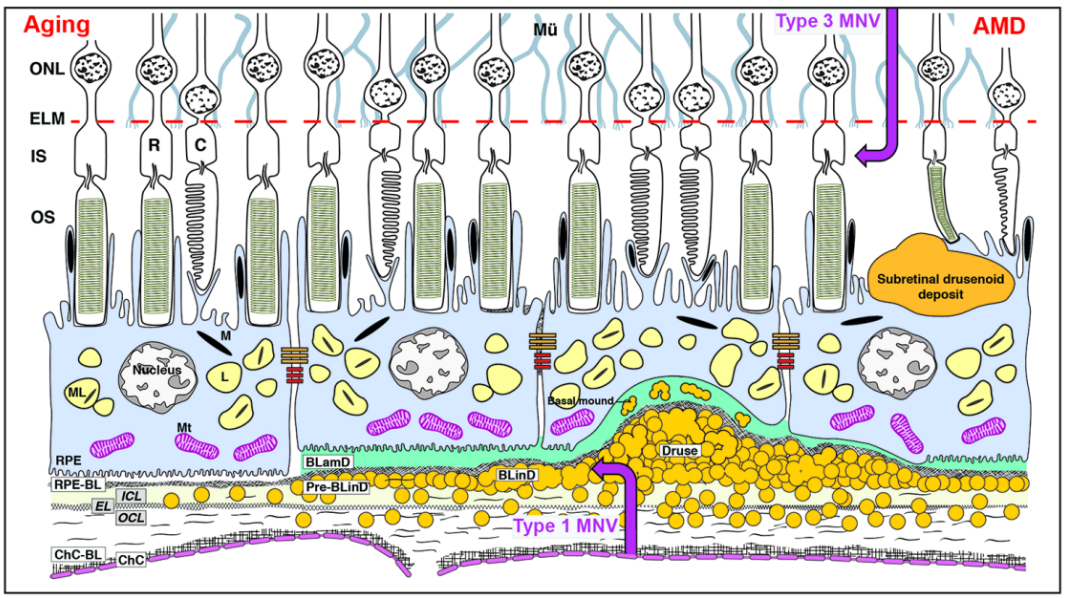


图1 眼底老化相关沉积物与外层视网膜结构关系示意图[14]

Figure1 Diagram illustrating the relationship between age-related fundus deposits and the outer retina[14]

BrM由RPE-BL、ICL、EL、OCL和ChC-BL五层结构构成。随着年龄增长，中性脂质(黄色圆圈)逐渐于BrM的EL及ICL中积聚，形成一层薄的脂质层(pre-BLinD)，并逐渐增厚形成BLinD，当脂质沉积进一步增多可形成呈局灶性分布的软性玻璃膜疣。中性脂质在BrM中的沉积使RPE-BL与BrM分离而形成一个潜在的RPE-BL下空间，1型MNV(紫色向上箭头)可侵入该区域，由此构成AMD进展及新生血管形成的病理解剖基础。BLamD是RPE-BL的弥漫性增厚(绿色)。SDD为位于RPE上方的沉积物，可致其上光感受器萎缩等改变，亦可极大增加3型MNV(紫色向下箭头)的患病风险。

缩写：BrM，布鲁赫膜；RPE，视网膜色素上皮；BL，基底膜；ICL，内胶原层；EL，弹力层；OCL，外胶原层；ChC，脉络膜毛细血管；pre-BLinD，基底线性沉积物前体；BLinD，基底线性沉积物； MNV，黄斑新生血管；AMD，年龄相关性黄斑变性；BLamD，基底薄层沉积物；SDD，视网膜下玻璃膜疣样沉积物； ONL，外核层；ELM，外界膜；IS，光感受器内节；OS，光感受器外节；Druse，玻璃膜疣

Bruch's membrane (BrM) consists of five layers of connective tissue: RPE-BL, ICL, EL, OCL, and ChC-BL. With aging, neutral lipids (yellow circles) gradually accumulate within the EL and ICL of BrM, forming a thin layer of lipid wall known as pre-BLinD, which gradually progressed to BLinD. As lipid deposition further increases, soft drusen, which are focal deposits of the same lipoprotein-derived debris as the BLinD, may form. The accumulation of neutral lipids in BrM results in the separation of RPE-BL from BrM, creating a potential sub-RPE-BL space. Type 1 MNV (purple upward arrow) can invade into this space, as a pathological and anatomical basis for the progression of AMD and neovascularization. Additionally, diffuse thickening of the RPE-BL, known as BLamD (highlighted in green), also may exacerbate retinal dysfunction. SDD, deposited above the RPE, can lead to photoreceptor atrophy and significantly increase the risk of type 3 MNV (purple downward arrow).

Abbreviations: BrM, Bruch's membrane; RPE, retinal pigment epithelium; BL, basal lamina; ICL, inner collagenous layer; EL, elastic layer; OCL, outer collagenous layer; ChC, choriocapillaris; pre-BLinD, precursor to basal linear deposits; BLinD, basal linear deposits; MNV, macular neovascularization; AMD, age-related macular degeneration; BLamD, basal laminar deposits; SDD, subretinal drusenoid deposits; ONL, outer nuclear layer; ELM, external limiting membrane; IS, photoreceptor inner segment; OS, photoreceptor outer segment.

分(图2B)。在超微结构上，早期 BLamD类似于RPE基底膜组织，而后期BLamD表现得更均匀致密[25]。如果BLamD厚度超过眼底光学相干断层扫描成像(optical coherence tomography, OCT)的分辨率，可能显示为OCT上的“双层征”，即RPE与BrM分离(图2 C、D)[23]。由于早中期AMD患者中有近10%~15%会出现新生血管性AMD (neovascular age-related macular degeneration, nAMD)，特别是1型黄斑新生血管(macular neovascularization, MNV)形成[26]，而1型MNV在OCT上表现为典型的“双层征”(图2 E、F)[13]，因此临床上需注意二者鉴别。近年来发现，利用超高分辨率光谱域-OCT (ultra-high-resolution spectral domain optical coherence tomography, UHR-SD-OCT)可以弥补传统OCT成像无法区分BLamD和BLinD的不足，发现BLamD的平均厚度约为BLinD的3倍[27]。从机制上而言，BLamD可能促进脂质等代谢物向BrM内胶原层的输送，参与了BLinD及软性玻璃膜疣的形成[16]。

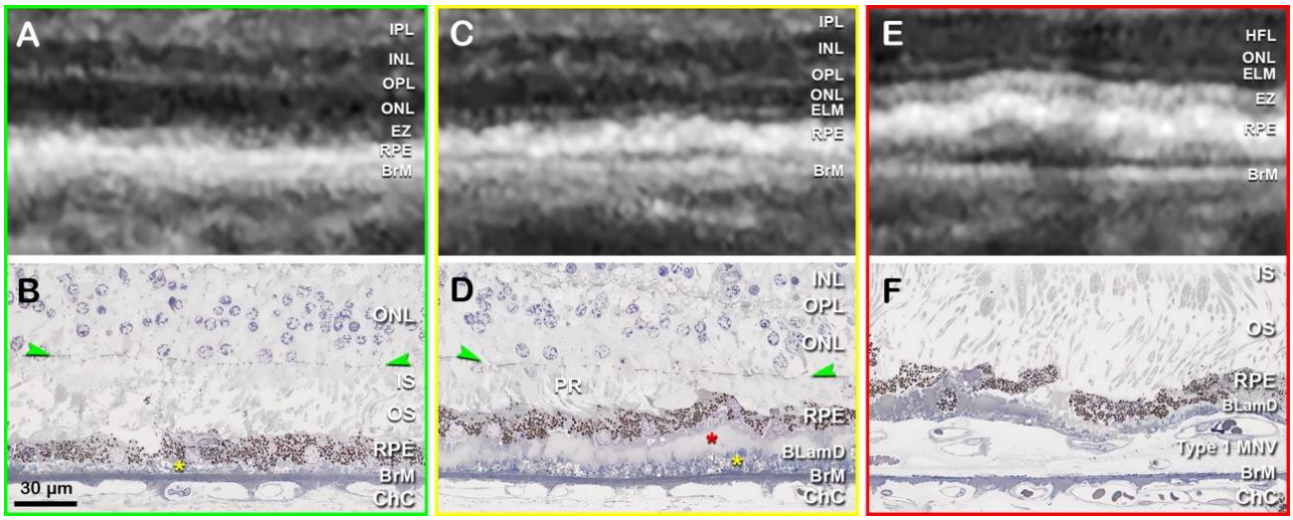


图2　BLamD与1型MNV的临床组织病理学相关性[24]

Figure 2　Clinicopathologic correlation of BLamD and Type 1 MNV[24]

A和B，C和D，以及E和F代表了OCT及相应的组织病理学图像。(A) OCT无法显示薄的BLamD；(B) 组织病理学显示RPE下非常薄的早期BLamD(黄色星号)；(C) OCT显示RPE光带增厚，反射增强，其与BrM间可见低反射(形似分离)；(D) 组织病理学显示RPE下非常厚的BLamD，包括早期BLamD(黄色星号)和晚期BLamD(红色星号)；(E) OCT显示RPE光带明显增厚，反射增强，其与BrM间分离；(F) 组织病理学显示RPE和BrM间的1型 MNV。

缩写：OCT，光学相干断层扫描成像；BLamD，基底薄层沉积物；RPE，视网膜色素上皮；BrM，布鲁赫膜；MNV，黄斑新生血管；IPL，内丛状层；INL，内核层；OPL，外丛状层；HFL，亨利纤维层；ONL，外核层；ELM，外界膜；EZ，椭球区；IS，光感受器内节；OS，光感受器外节；ChC，脉络膜毛细血管

A and B, C and D, as well as E and F represent OCT and the corresponding histopathological images. (A) OCT cannot reveal the presence of thin BLamD; (B) Histopathology findings show very thin early BLamD beneath the RPE (yellow asterisk); (C) OCT displays the RPE band thickening with reflectivity enhanced, and a hyporeflective space resembling separation between it and BrM; (D) Histopathology findings demonstrate markedly thick BLamD under the RPE, including early BLamD (yellow asterisk) and late BLamD (red asterisk); (E) OCT shows significant thickening of the RPE band with enhanced reflectivity and separation from BrM, i.e double-layer sign; (F) Histopathology findings reveal Type 1 MNV between the RPE-BL and BrM.

Abbreviations: OCT, optical coherence tomography; BLamD, basal laminar deposit; RPE, retinal pigment epithelium; BrM, Bruch's membrane; MNV, macular neovascularization; IPL, inner plexiform layer; INL, inner nuclear layer; OPL, outer plexiform layer; HFL, Henle fiber layer; ONL, outer nuclear layer; ELM, external limiting membrane; EZ, ellipsoid zone; IS, photoreceptor inner segment; OS, photoreceptor outer segment; ChC, choriocapillaris.

2.2　Pre-BLinD/BLinD及软性玻璃膜疣

随着患者年龄的增长，BrM弹力层和内胶原层间逐渐发生物质沉积。这些沉积物由多种脂质(主要为酯化和未酯化胆固醇)、蛋白质(β淀粉样蛋白、补体因子和玻连蛋白等)、碳水化合物和无机物(钙、铁、锌和羟基磷灰石等)构成，其中脂质占总成分的40%～50%[2,28]。这些位于RPE基底膜下以疏水中性脂质为主的沉积物早期呈弥漫性分布，被称为Pre-BLinD/BLinD(图3A、B)，后期可呈局灶性分布，即为软性玻璃膜疣(图3C)[2]。Pre-BLinD/BLinD及软性玻璃膜疣是同一沉积物在RPE基底膜下空间不同形式的沉积，由于在透射电镜下呈卷曲膜样的超微结构，因此最初报道其主要由膜样残骸构成[29]。Curcio教授团队采用锇鞣酸对苯二胺(osmium tannic acid paraphenylenediamine, OTAP)后固定的细胞外脂质保存技术[28]，更好地显示并深入研究了这类沉积物，证明其由富含酯化和未酯化胆固醇的中性脂质构成，而并非来自膜样残骸，且Pre-BLinD/BLinD和软性玻璃膜疣均为早期AMD特异性的病理改变，与AMD的发生及进展密切相关[30]。在人成年早期，中性脂质开始在BrM弹力层沉积，随着年龄增长逐渐增多而累及内胶原层，最终在内胶原层与RPE基底膜之间形成致密的脂质层，导致BrM疏水性增加[31]。这一脂质沉积过程同样发生在周边视网膜，只不过脂质沉积的速度更慢，研究证明黄斑区脂质沉积约为周边视网膜的7倍[32]。随后氧化及非氧化反应导致其内载脂蛋白降解和颗粒融合，促使Pre-BLinD /BLinD及软性玻璃膜疣的形成[33]。这些沉积物在干性AMD眼中普遍

存在，使得黄斑区RPE基底膜与BrM内胶原层之间分离形成一个潜在的RPE基底膜下空间(图1)，构成了AMD进展及新生血管形成的病理解剖基础。

Pre-BLinD/BLinD和软性玻璃膜疣的病因复杂，补体、慢性氧化应激、炎症反应、缺氧、线粒体功能障碍、自噬受损及脉络膜毛细血管萎缩等都可能与之密切相关[8,34-36]，而RPE细胞的胆固醇代谢失调对这些沉积物的形成和积聚至关重要[37-38]。有研究表明，参与胆固醇代谢和转运相关蛋白，如ATP结合盒转运蛋白A1 (ATP-binding cassette transporter A1, ABCA1)能够促进RPE细胞向其顶端的光感受器以及其基底端外排胆固醇[39]，过氧化物酶体增殖物激活受体γ (peroxisome proliferator activated receptor gamma, PPARG)基因、血管生成素样蛋白3 (angiopoietin-like protein 3, ANGPTL3)基因、N-脱乙酰酶和N-磺基转移酶1 (N-deacetylase and N-sulfotransferase 1, NDST1)基因以及线粒体甘油-3-磷酸乙酰转移酶 (mitochondrial glycerol-3-phosphate acyltransferase, GPAM)基因等参与了脂蛋

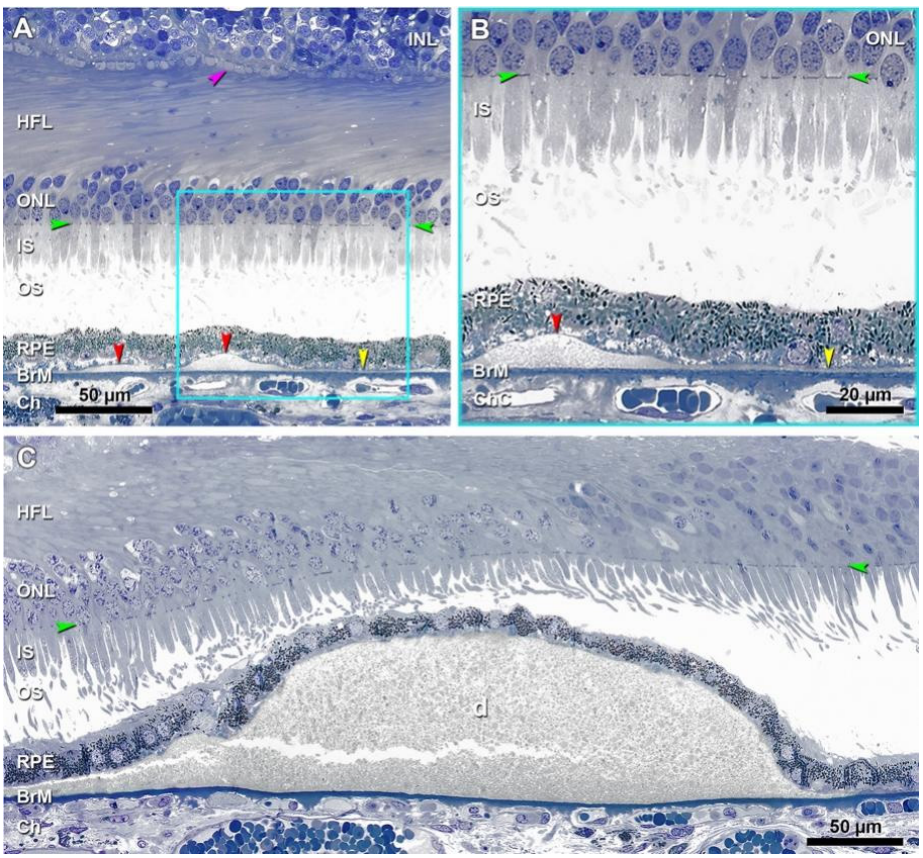


图3 Pre-BLinD/BLinD及软性玻璃膜疣的组织病理学特征[14]

Figure 3 Histopathological characteristics of pre-BLinD/BLinD and soft drusen[14]

(A和B) Pre-BLinD(黄色箭头)和BLinD(红色箭头)为RPE-BL与BrM间弥散性颗粒状沉积，且位于同一RPE-BL下空间；(C) 软性玻璃膜疣；(D) 位于黄斑区RPE-BL与BrM之间，呈浅灰色颗粒状沉积，与Pre-BLinD/BLinD成分相同，其上RPE隆起，厚度稍变薄，上方OS明显缩短。

缩写：Pre-BLinD，基底线性沉积物前体；BLinD，基底线性沉积物；RPE，视网膜色素上皮；BL，基底膜；BrM，布鲁赫膜；OS，光感受器外节；INL，内核层；HFL，亨利纤维层；ONL，外核层；IS，光感受器内节；Ch，脉络膜；ChC，脉络膜毛细血管

(A and B) Pre-BLinD (yellow arrowhead) and BLinD (red arrowhead) represent diffuse, granular deposits between the RPE-BL and BrM; (C) Soft drusen (D) mainly in the macular region, appearing as light gray granular deposits between the RPE-BL and BrM, with the same lipoprotein-derived debris as Pre-BLinD/BLinD. The overlying RPE layer demonstrates a dome-shaped elevation and reduced thickness, while the OS above is markedly shortened.

Abbreviations: Pre-BLinD, precursor to basal linear deposits; BLinD, basal linear deposits; RPE, retinal pigment epithelium; BL, basement membrane; BrM, Bruch's membrane; OS, photoreceptor outer segment; INL, inner nuclear layer; HFL, Henle fiber layer; ONL, outer nuclear layer; IS, photoreceptor inner segment; Ch, choroid; ChC, choriocapillaris.

白代谢的转录后调控[40]，在载脂蛋白E (apolipoprotein E, APOE)基因、胆固醇酯转移蛋白(cholesteryl ester transfer protein, CETP)基因、ABCA1基因和肝脂肪酶C (lipase C, LIPC)基因等脂质代谢基因中发现了与晚期AMD相关的单核苷酸多态性(single nucleotide polymorphism, SNP)[41-43]。此外，自噬作为一种细胞稳态调节途径，当功能受损后可观察到RPE细胞内脂褐素累积和细胞外沉积物增多[40]。

2.2.1 Pre-BLinD/BLinD的病理特征及多模态影像学表现

由于BLinD在透射电镜下呈卷曲膜样的超微结构，因此最初被认为是一些膜样残骸[29]，经后续研究发现，它主要是一种厚度约为0.4~2.0 μm、薄而致密的中性脂质沉积层，病理学上表现为细颗粒状较均匀的沉积物[44-45]，Pre-BLinD为其前体(图3A、B)。Pre-BLinD/BLinD为亚临床病理改变，既往研究表明其无法在体内通过彩色眼底照相(color fundus photography, CFP)、荧光素眼底血管造影(fundus fluorescein angiography, FFA)、眼底自发荧光(fundus autofluorescence, FAF)及OCT等手段检测，而只能在病理上被显示(图4E，红色箭头)[46]，因此对其临床意义的理解相对局限。文峰教授团队通过临床系列研究首次在国际上证明Pre-BLinD/BLinD可在吲哚菁绿血管造影(indocyanine green angiography, ICGA)后期被观察到，表现为ICGA后期年龄相关性弱荧光斑(age-related scattered hypofluorescent spots on late-phase indocyanine green angiography, ASHS-LIA)，而在CFP、FFA、OCT及FAF上均无相应表现[46-48]。通过对高分辨率光学显微镜下表现和临床病理学的相关性分析，发现Pre-BLinD/BLinD对比软性玻璃膜疣而言具有更广泛的眼底覆盖面积(前者约为后者的1.9~3.4倍)[49]，可极大增加AMD的疾病进展风险。值得注意的是，息肉状脉络膜血管病变(polypoidal choroidal vasculopathy, PCV)患者的ASHS-LIA检出率最高，且ASHS-LIA可增加其双侧发病风险[47]。PCV为nAMD在亚洲的主要亚型，目前认为其是1型MNV的变型，因此又被称为动脉瘤1型MNV[50]，通常以不伴有软性玻璃膜疣的视网膜色素上皮异常为特征[51-52]。基于此，文峰教授团队推测Pre-BLinD/BLinD可能作为PCV的先兆病变发挥致病作用，并在国际上首次提出BLinD参与PCV发病机制假说[51]，这也合理解释了为什么区别于典型nAMD，PCV患者通常不伴有软性玻璃膜疣，而以视网膜色素上皮异常为特征。

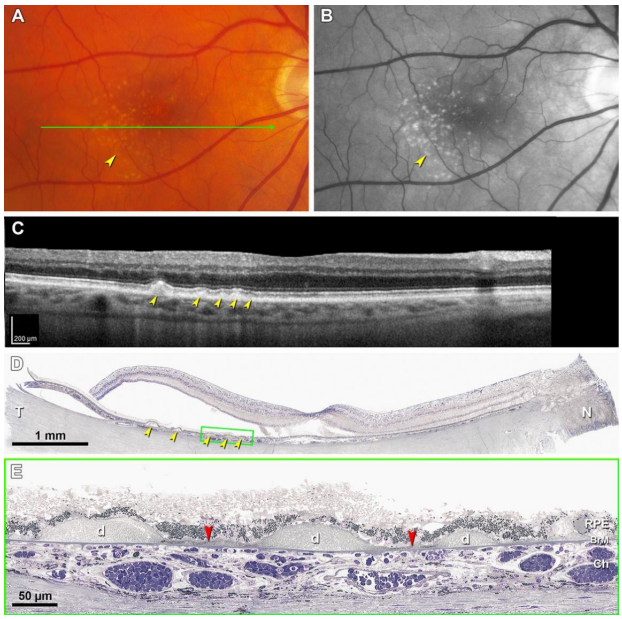


图4　BLinD及软性玻璃膜疣的多模态影像及临床病理相关性[14]

Figure 4　Multimodal imaging and clinicopathologic correlation of BLinD and soft drusen[14]

(A) CFP上可见位于黄斑颞下方的黄白色点状玻璃膜疣；(B) 无赤光眼底照相下玻璃膜疣显示更加清晰；(C) 对应于A图中绿色线条处OCT显示玻璃膜疣呈局灶性山丘状或驼峰状RPE隆起，伴下方中等反射沉积物；(D) 与OCT相对应的组织病理图像显示数个软性玻璃膜疣(黄色箭头)；(E) 显示了D图中绿色框区域的放大图像，可见BLinD(红色箭头)和软性玻璃膜疣(d)分别是相同物质的弥散性和局灶性沉积，位于同一RPE-BL下空间。

缩写：BLinD，基底线性沉积；CFP，彩色眼底照相；OCT，光学相干断层扫描；RPE，视网膜色素上皮；BL，基底膜

(A) CFP shows yellowish-white dot-like drusen deposited in the temporal region of the macula; (B) Soft drusen are clearly visible under red-free image; (C) OCT B-scan at the green arrow line in A demonstrates soft drusen as focal hill-like or hump-like elevations of the RPE, accompanied by medium reflective deposits underneath; (D) Histopathological findings corresponding to the OCT B-scan reveal several soft drusen (yellow arrowhead); E. Magnified image of the green box area in D shows BLinD (red arrowhead) and soft drusen (d), which represent diffuse and focal deposits of the same material, both located in the same sub-RPE-BL space.

Abbreviations: BLinD, basal linear deposit; CFP, color fundus photography; OCT, optical coherence tomography; RPE, retinal pigment epithelium; BL, basement membrane.

2.2.2 软性玻璃膜疣的病理特征及多模态影像学表现

软性玻璃膜疣是在Pre-BLinD/BLinD的基础上，脂质沉积进一步增多，呈局灶性分布而形成(图3C，图4D、E)。与Pre-BLinD/BLinD的分布相似，软性玻璃膜疣主要分布于黄斑区，位于RPE基底膜与BrM内胶原层之间，是AMD疾病进展最重要的风险因素[18]。

既往研究表明，软性玻璃膜疣的数量和大小与AMD的疾病进展呈正相关性，与典型nAMD发生亦密切相关[53]。根据大小可将玻璃膜疣分为小玻璃膜疣、中等玻璃膜疣和大玻璃膜疣，小玻璃膜疣直径<63 μm，中等玻璃膜疣直径为63~125 μm，大玻璃膜疣直径≥125 μm[1]。根据玻璃膜疣的大小和性状、视网膜色素上皮改变情况、有无新生血管或萎缩对AMD进行Beckman分类，可分为早期、中期和晚期AMD(现称为进展期AMD)[54]。利用眼底多模态影像学手段有助于软性玻璃膜疣的检出，其在CFP上表现为位于黄斑区的黄白色类圆形沉积物，呈“柔软样外观”，边界欠清可融合，可伴有色素紊乱(图5A)，且分布密度以黄斑为中心向外逐渐降低[18, 55]。软性玻璃膜疣在FAF上根据对光感受器及RPE损害程度的不同可呈现不同的自发荧光表现[56]；其在FFA上可呈现多样化改变，无特异性，多表现为RPE色素脱失所致透见荧光，也可表现为荧光素着染所致强荧光，但无荧光素渗漏现象(图5B)；其在ICGA上表现为弱荧光，在ICGA晚期表现为密集的弱荧光，周围常伴有ASHS-LIA的稍弱荧光斑(图5C)。OCT上软性玻璃膜疣表现为RPE下局灶性山丘状或驼峰状的中等反射沉积物(图5D)[57-58]。研究表明，软性玻璃膜疣是动态变化的，在发生后的5～7年内，20%～34%会自行消失[59-60]。而持续生长的软性玻璃膜疣最终可进展至1型MNV或2型MNV，也可进展为地图样萎缩(geographic atrophy, GA)[18]。此外，软性玻璃膜疣逐渐增大可形成玻璃膜疣样色素上皮脱离(drusenoid pigment epithelial detachment, PED)，造成其上RPE迁移

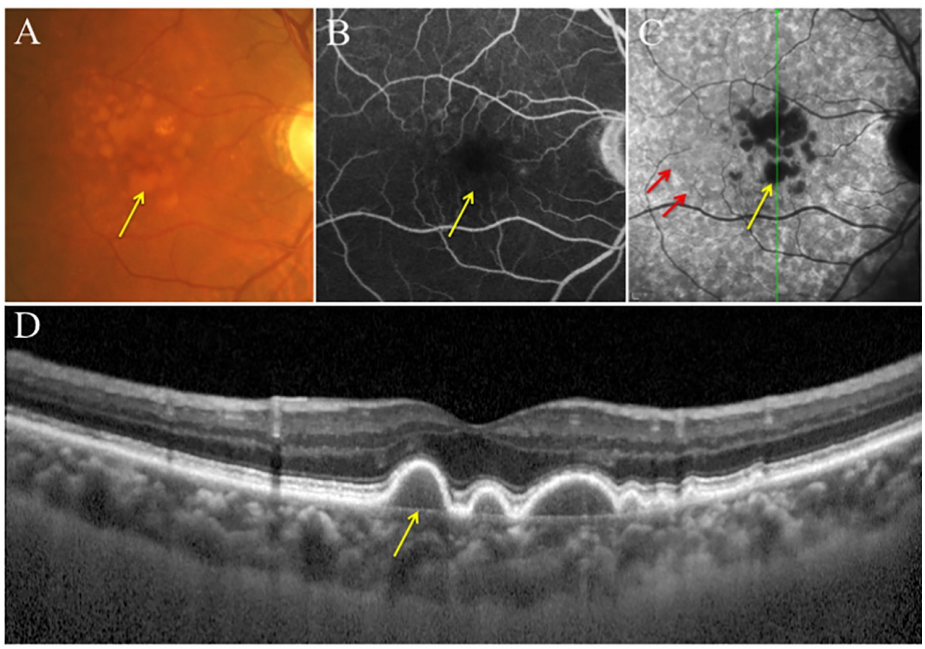


图5 软性玻璃膜疣的多模态影像学特征[48]

Figure 5 Multimodal imaging characteristics of soft drusen [48]

(A) CFP上可见黄斑区大量黄白色脂质沉积物(黄色箭头)，边界欠清，局部融合，伴眼底色素紊乱；(B) FFA显示与软性玻璃膜疣位置相对应的轻度高荧光斑(黄色箭头)；(C) ICGA晚期可见软性玻璃膜疣呈密集低荧光斑，部分融合(黄色箭头)，周围绕以ASHS-LIA稍弱荧光斑(红色箭头)；(D) 对C图中的绿线处进行OCT扫描，显示RPE呈山丘状或驼峰状隆起，伴其下中等反射沉积物(黄色箭头)。

缩写：CFP，彩色眼底照相；FFA，荧光素眼底血管造影；ICGA，吲哚菁绿血管造影；ASHS-LIA，年龄相关性吲哚菁绿血管造影晚期散在低荧光斑点；OCT，光学相干断层扫描

(A) CFP shows substantial yellow-white drusen-like material deposited in the macular region (yellow arrow), with unclear boundaries, partial fusion, as well as fundus pigment disorder; (B) FFA displays mild hyperfluorescence corresponding to the soft drusen (yellow arrow); (C) Late-phase ICGA reveals dense hypofluorescent spots of soft drusen, some of which have merged (yellow arrow), surrounded by ASHS-LIA (red arrow); (D) OCT B-scan at the green line in C shows that the RPE is elevated in a hill-like or hump-like manner, with medium-reflective deposits underneath (yellow arrow).

Abbreviations: CFP, color fundus photography; FFA, fluorescein fundus angiography; ICGA, indocyanine green angiography; ASHS-LIA, age-related scattered hypofluorescent spots on late phase indocyanine green angiography; OCT, optical coherence tomography.

或萎缩，进而PED坍塌，导致GA的发生[18,61-62]。

2.3　硬性玻璃膜疣

硬性玻璃膜疣通常较小(直径<63 μm)，于眼底后极部特别是周边视网膜散在分布[63]。正常的老化眼底常观察到硬性玻璃膜疣，但较多(≥20个)这类沉积物的出现可能预示着早期AMD的发生和进展[64]。与软性玻璃膜疣一样，硬性玻璃膜疣亦位于RPE基底膜与BrM之间，但其在眼底的分布与软性玻璃膜疣不同。组织病理学显示硬性玻璃膜疣为质地致密，球型或半球形，染色均匀的沉积物，其上RPE层可变薄或萎缩(图6)。

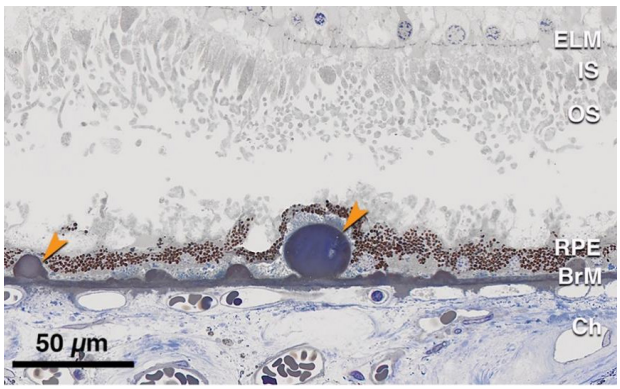


图6　硬性玻璃膜疣的组织病理学特征

Figure 6　Histopathological features of hard drusen

硬性玻璃膜疣位于RPE-BL与BrM之间，为球形或半球形的致密沉积物，组织病理学上染色均匀，其上RPE被顶起，局部变薄，下方BrM连续。

缩写：RPE，视网膜色素上皮；BL，基底膜；BrM，布鲁赫膜

Hard drusen are deposited between the RPE-BL and BrM, appearing as spherical or hemispherical dense deposits. Histopathologically, they stain uniformly, with the RPE elevated and thinned above and the BrM continuous underneath.

Abbreviations: RPE, retinal pigment epithelium; BL, basal lamina; BrM, Bruch's membrane.

临床上多种手段可用于检测硬性玻璃膜疣，其在检眼镜和CFP上表现为离散的黄白色点状沉积物，边界清楚，常伴色素改变(图7A)[64]。FFA上硬性玻璃膜疣表现为RPE色素脱失所致透见荧光(图7B)；ICGA晚期硬性玻璃膜疣表现为点状染色性强荧光，且位于ASHS-LIA的弱荧光范围之外，使ASHS-LIA显影更清楚(图7C、D)；OCT上硬性玻璃膜疣表现为RPE下点状高反射沉积物(图7F)[65]。除了见于老化的眼底，硬性玻璃膜疣在年轻人眼底也很常见。研究表明，有超过90%的20～46岁健康成年人和约11%的11～12岁健康儿童在接受眼底检查时观察到硬性玻璃膜疣[66-67]。近年来，利用自适应光学扫描检眼镜(adaptive optics scanning laser ophthalmoscopy, AO-SLO)检测到这些玻璃膜疣呈直径为22~61 μm的圆形或椭圆形分布，对应于1~4个RPE 细胞的大小，两个或多个较小病灶可融合形成小叶型硬性玻璃膜疣，其上视锥细胞密度和反射率降低[65]。

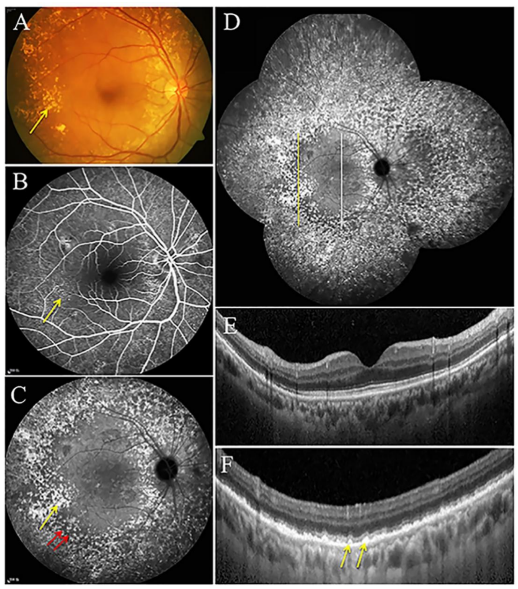


图7　硬性玻璃膜疣的多模态影像学特征[48]

Figure 7　multimodal imaging features of hard drusen[48]

(A) CFP上可见后极部大量黄白色点状沉积物，边界清晰锐利(黄色箭头)；(B) FFA 显示大量与A中沉积物位置相对应的点状强荧光(黄色箭头)；(C) ICGA晚期显示沉积物染色呈强荧光(黄色箭头)，且位于ASHS-LIA弱荧光区域外(红色箭头)；(D) ICGA晚期拼图显示硬性玻璃膜疣与ASHS-LIA的分布关系；(E) 对D图中的白线处进行OCT扫描，显示未观察到与ASHS-LIA对应的变化；(F) 对D图中的黄线处进行OCT扫描，显示位于RPE下方的多发局灶性高反射沉积物(黄色箭头)。

缩写：CFP，彩色眼底照相；FFA，荧光眼底血管造影；ICGA，吲哚菁绿血管造影；ASHS-LIA，年龄相关性吲哚菁绿血管造影晚期散在低荧光斑点；OCT，光学相干断层扫描；RPE，视网膜色素上皮

(A) CFP shows numerous yellow-white punctate deposits with well-defined, sharp borders in the posterior pole (yellow arrow); (B) FFA shows lots of hyperfluorescent spots corresponding to the deposits in A (yellow arrow); (C) Late-phase ICGA demonstrates hyperfluorescent staining of the deposits (yellow arrow) located outside the hypofluorescent area of ASHS-LIA (red arrow); (D) The merged image of late-phase ICGA shows the distribution of hard drusen and ASHS-LIA; (E) OCT B-scan (the white line in D), revealing no changes corresponding to the ASHS-LIA are observed; (F) OCT B-scan (the yellow line in D) displays multiple focal hyperreflective deposits underneath the RPE (yellow arrows).

Abbreviations: CFP, color fundus photography; FFA, fundus fluorescein angiography; ICGA, indocyanine green angiography; ASHS-LIA, age-related scattered hypofluorescent spots on late phase indocyanine green angiography; OCT, optical coherence tomography; RPE, retinal pigment epithelium.

2.4 表皮玻璃膜疣

表皮玻璃膜疣被认为是RPE基底膜局灶性结节状增厚的结果，在检眼镜和CFP下与硬性玻璃膜疣的表现相似，呈离散分布的类圆形黄白色点状沉积，大小均匀，直径约为25~75 μm[68](图8A)。对比硬性玻璃膜疣，表皮玻璃膜疣在眼底的数量更多且密度更高，为RPE基底膜下实性沉积物。它们散布整个眼底，通常聚集在后极部[69-70]。表皮玻璃膜疣在FFA上表现为大量分散且大小均匀的点状透见荧光，双眼对称分布，该现象通常被描述为“满天星”[68,70](图8B)。与软性玻璃膜疣类似，表皮玻璃膜疣在FAF上根据其对光感受器及RPE损害程度的不同可呈不同的自发荧光表现[56]。OCT上可见典型的“锯齿样”高反射沉积物，较大的病灶呈山丘状隆起，由于其上RPE萎缩引起的信号透见可在脉络膜区域形成特征性的“条形码”外观[69]。组织病理显示表皮玻璃膜疣为位于RPE基底膜下实性沉积物，质密且染色均匀(图8C)，其随年龄增长可逐渐扩大融合，呈颗粒状外观，后期与软性玻璃膜疣难以区分(图8D~G)。

表皮玻璃膜疣被认为是一种早发型玻璃膜疣，通常在50岁之前被诊断出来，它们与AMD的发生和发展风险无关，虽然早期无特殊症状，但晚期病变发生广泛融合后可导致一系列病理改变，增加视网膜萎缩和新生血管形成的风险[68]。此外，表皮玻璃膜疣是否会对视觉功能产生影响目前存在争议。Goh等[72]的研究发现它们与未来3年内患进展期AMD的风险性无关，且不伴有视觉敏感度下降[72]。Charng等[73]通过眼底多模态成像和微视野测定证明表皮玻璃膜疣的出现不影响视网膜敏感性[73]。与之相反，Nam等[74]认为3型表皮玻璃膜疣(直径> 200 μm)与视网膜敏感性显著降

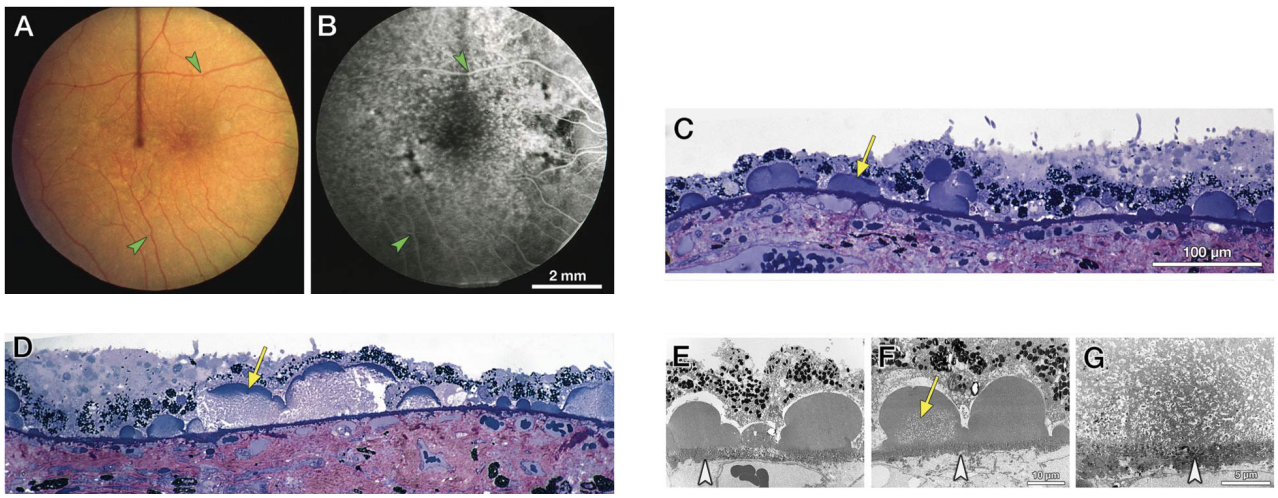


图8 表皮玻璃膜疣的眼底表现及组织病理学特征[71]

Figure 8 Fundus manifestations and histopathological characteristics of cuticular drusen[71]

(A) CFP上，表皮玻璃膜疣为散在分布的浅淡黄白色类圆形点状沉积物，大小较均匀；(B) FFA上，表皮玻璃膜疣表现为大量点状透见荧光，似“满天星”；(C) 组织病理学显示大量分散的RPE-BL下实性沉积物(黄色箭头)，质密，染色均匀；(D) 部分表皮玻璃膜疣发生融合(黄色箭头)，其外部染色质密，内部呈颗粒状外观；(E、F和G)了表皮玻璃膜疣在透射电子显微镜下的超微结构，白色箭头示BrM；(E) 成熟表皮玻璃膜疣，电子密度适中，内部均匀；(F) 处于形成阶段的表皮玻璃膜疣，黄色箭头处为电子密度稍低的较疏松区域；(G) 放大后的表皮玻璃膜疣，可见背景均匀，含多个散在的电子致密小球，和脂质的表现类似。

缩写：CFP，彩色眼底照相；FFA，荧光眼底血管造影；RPE，视网膜色素上皮；BL，基底膜；BrM，布鲁赫膜

(A) On CFP, cuticular drusen appear as scattered yellow-white punctate deposits, uniform in size; (B) On FFA, cuticular drusen manifest as numerous punctate hyperfluorescence in a canonical “starry sky” pattern; (C) Histopathological findings reveal lots of solid deposits beneath the RPE-BL (yellow arrow), with a solid homogeneous appearance; (D) Some cuticular drusen can be confluent (yellow arrow), with a dense staining contour and a granular appearance internally; (E, F, and G) The ultrastructure of cuticular drusen under transmission electron microscopy, with BrM indicated by white arrowhead; (E) Mature cuticular drusen with moderate electron density and homogenous internal structure; F. Cuticular drusen in the formation stage, with the yellow arrow indicating a slightly lower electron density and a looser region; (G) Magnified image of cuticular drusen with a uniform background containing multiple scattered electron-dense granules, resembling lipid-like deposits.

Abbreviations: CFP, color fundus photography; FFA, fundus fluorescein angiography; RPE, retinal pigment epithelium; BL, basal lamina; BrM, Bruch's membrane.

低有关[74]。因此，表皮玻璃膜疣的病理生理作用还有广阔的研究空间，相关研究成果有助于为临床上检出该病变的个体制定更合理的监测策略。

2.5 SDD

SDD，既往又被称为网状假性玻璃膜疣(reticular pseudodrusen, RPD)，是一种主要见于黄斑中心凹旁和视盘旁，且较少累及中心凹的多发黄色点状沉积物，可融合成分支状或网状[75]。Curcio教授团队通过病理研究证实这种沉积物位于神经视网膜下，因此将之命名为视网膜下玻璃膜疣样沉积物SDD。SDD在组织病理学上表现为呈细颗粒状的细胞外沉积(直径可小至4 μm)，其发生于RPE顶端并定位在RPE和光感受器之间，可致其下RPE局部萎缩变薄，其上光感受器内外节缩短(图9A)，且SDD表面可堆积脱落的OS(图9B)，随着SDD逐渐增大可突破外界膜[14-15]。SDD中富含RPE细胞及OS组分，其蛋白成分与软性玻璃膜疣类似(含ApoE、补体因子H和玻连蛋白等；SDD中ApoB和ApoA-I等含量较低)，但脂质成分与后者相比有较大不同，SDD主要以游离胆固醇等极性脂质沉积为主且不含胆固醇酯，而软性玻璃膜疣二者皆含，此外，在软性玻璃膜疣中常见的羟基磷灰石样折光性小体在SDD中并不易观察到[75-76]。因此，不能单纯认为SDD是位于RPE顶端的玻璃膜疣，二者在组成成分和形成机制上存在差异。有研究表明，RPE缺氧、RPE脂质转运机制异常、RPE极性丧失以及维生素A或类维生素A循环异常均有可能参与了SDD的发病机制[75,77]。另外，SDD通常伴随着由视杆细胞介导的视力下降，表现为暗适应功能受损最为明显，这也与其较少累及以视锥细胞为主的黄斑中心凹，而是累及以视杆细胞为主的中心凹旁及其周围视网膜相对应[78]。由于两种光感受器外节的脂质类型不同，SDD可能与反应视杆细胞的外层视网膜脂质循环系统受损有关[75]。

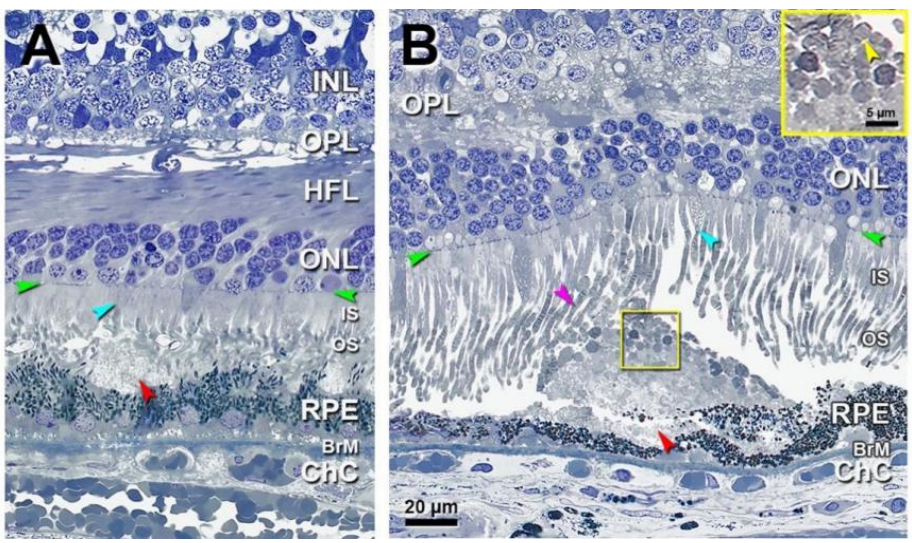


图9 SDD的组织病理学特征[79]

Figure 9 Histopathological features of SDD[79]

(A) SDD为位于RPE上方的“土堆样”细颗粒状沉积物，其下方RPE局部变薄，上方的OS缩短；(B) 较大的“土堆样” 颗粒状沉积物位于RPE上方，其下RPE厚度不均，上方OS缩短、部分发生偏转(紫红色箭头)，部分IS亦缩短(蓝绿色箭头)，沉积物表面可见脱落堆积的OS，在顶部形成帽状结构(黄框及黄色箭头)。

缩写：SDD，视网膜下玻璃膜疣样沉积物；RPE，视网膜色素上皮；OS，光感受器外节；IS，光感受器内节；INL，内核层；OPL，外丛状层；HFL，亨利纤维层；ONL，外核层；BrM，布鲁赫膜；ChC，脉络膜毛细血管

(A) SDDs are characterized by granular deposits presenting a “mound-like” appearance and located above the RPE, with the underlying RPE thinning and the overlying OS shortening; (B) Larger “mound-like” granular deposits are situated above RPE of very nonuniform thickness, with the underlying RPE uneven thinning, and the overlying OS shortened or partially deflected (purple-red arrowhead), while parts of the IS are also shortened (blue-green arrowhead). Detached and accumulated OS can be observed on the surface of the deposits, forming a cap-like structure on the surface (yellow box and yellow arrowhead).

Abbreviations: SDD, subretinal drusenoid deposits; RPE, retinal pigment epithelium; OS, photoreceptor outer segment; IS, photoreceptor inner segment; INL, inner nuclear layer; OPL, outer plexiform layer; HFL, Henle fiber layer; ONL, outer nuclear layer; BrM, Bruch’s membrane; ChC, choriocapillaris.

CFP上，SDD表现为眼底黄斑中心凹旁及其周围视网膜密集分布的黄白色点状沉积物，越远离黄斑直径增大(图10A)，较大的病灶可融合成带状、分支状，甚至网状[79]。但与玻璃膜疣相比，SDD显得更白更蓝，这一现象在无赤光眼底照相下表现得尤为明显(图10B)。SDD在FAF上主要表现为低自发荧光，与其对RPE中荧光物质的遮蔽有关(图10C)，近红外光成像(near-infrared imaging, NIR)也可用于检测SDD，表现为密集分布的弱反射颗粒样沉积物(图10D)，如果SDD突破了椭圆体带，可观察到弱反射环围绕强反射中心的现象，呈“靶心状”外观[80]。SDD在FFA上通常不表现出特异荧光，可显示轻度弱荧光[81]，亦可表现为点状强荧光。由于局部RPE萎缩以及SDD遮蔽等因素，SDD在ICGA上表现为多发点状弱荧光，造影后期弱荧光更加显著[81]。在OCT上，SDD表现为位于RPE上方的间断突起的中高反射沉积物，大的沉积物可呈丘状隆起，可向上推移椭圆体带甚至突破外界膜(图10E)[80,82]。SDD与进展期AMD显著相关，包括参与GA和MNV形成，是进展期AMD的独立危险因素[79, 83-84]。其中检测出SDD的患者中有近2/3会发展成MNV，尤其是3型MNV，即视网膜血管瘤样增生(retinal angiomatous proliferation, RAP)[78,85]。而在具有GA和3型MNV的患眼中，SDD的检出率可高达90%[85-86]。

3 小结及展望

眼底老化相关沉积物是随着年龄增长出现在外层视网膜的异常沉积。部分沉积物是视网膜功能减退的正常老化现象，而另一些沉积物的出现常伴随着眼底的病理改变，且与AMD的发生和进展密切相关。本文总结了几类常见眼底老化相关沉积物的组织病理学特征和多模态影像学表现，阐述了不同沉积物或同种沉积物的不同阶段所展示出的特征及临

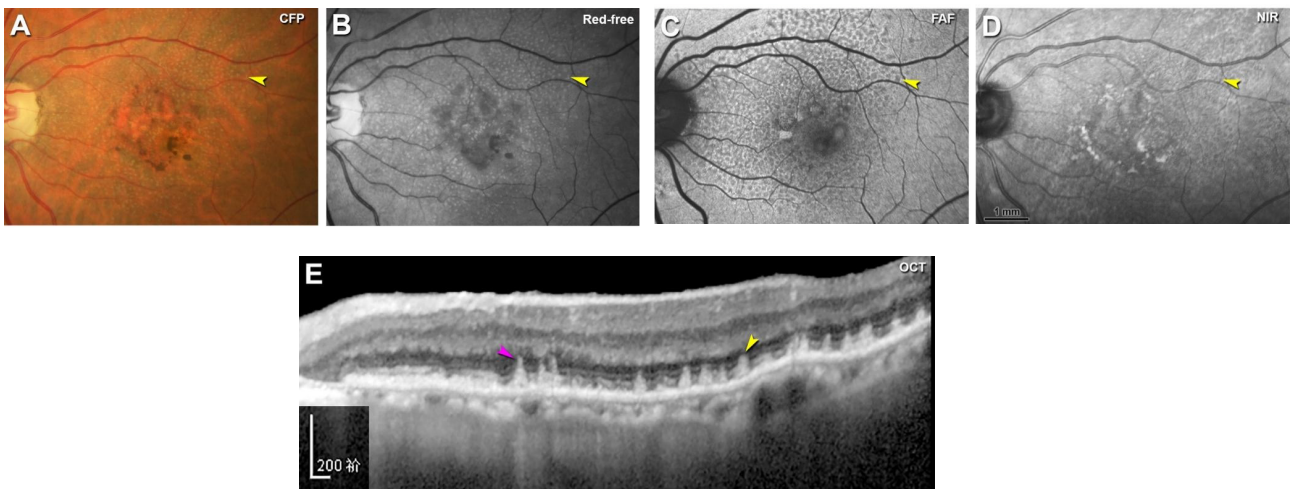


图10 SDD的多模态影像学特征

Figure 10 Multimodal imaging features of SDD

(A) CFP显示后极部大量黄白色点状沉积物，边界清晰，有立体感(黄色箭头)，黄斑区可见片状视网膜萎缩伴色素增生；(B) 无赤光眼底照相下点状沉积物清晰可见(黄色箭头)；(C) FAF上，SDD表现为斑点状低自发荧光，黄斑区可见卵黄样物质引起的高自发荧光及萎缩所致的低自发荧光；(D) NIR亦可显示点状的SDD沉积物，但欠清晰；E. OCT上，SDD表现为多发神经视网膜下中高反射沉积物(黄色箭头)，部分突破ELM进入ONL及OPL(紫红色箭头)。

缩写：SDD，视网膜下玻璃膜疣样沉积物；CFP，彩色眼底照相；FAF，眼底自发荧光；NIR，近红外光成像；OCT，光学相干断层扫描；ELM，外界膜；ONL，外核层；OPL，外丛状层

(A) CFP shows numerous yellow-white punctate deposits in the posterior pole (yellow arrowhead), with well-defined borders and a three-dimensional appearance. Patchy retinal atrophy and hyperpigmentation can be observed in the macular region; (B) The punctate deposits are clearly visible on red-free image (yellow arrowhead); (C) On FAF, SDD appear as speckled hypoautofluorescence, with high autofluorescence due to vitelliform material and low autofluorescence caused by atrophy in the macular region; (D) On NIR, punctate SDD also can be observed with less clarity; (E) On OCT B-scan, SDD manifest as multiple medium-reflective or high-reflective deposits located under the neurosensory retina (yellow arrowhead), with some of them breaking through the ELM and extending into the ONL and OPL (purple-red arrowhead).

Abbreviations: SDD, subretinal drusenoid deposits; CFP, color fundus photography; FAF, fundus autofluorescence; NIR, near-infrared imaging; OCT, optical coherence tomography; ELM, external limiting membrane; ONL, outer nuclear layer; OPL, outer plexiform layer.

床意义。脂质代谢紊乱在眼底老化相关沉积物的形成过程中扮演着至关重要的角色，特别是以酯化或未酯化胆固醇等中性脂质为主要成分的Pre-BLinD/BLinD和软性玻璃膜疣是AMD发生和进展最重要的病理基础，其中Pre-BLinD/BLinD是我国最常见nAMD亚型PCV的先兆病变，而软性玻璃膜疣常可进展为GA或典型nAMD。另一类重要的沉积物SDD与3型MNV发生发展密切相关。因此，探索脂质和胆固醇代谢异常在早期AMD中的启动机制有助于为疾病的干预和治疗找到新的突破口。此外，RPE基底膜下的玻璃膜疣样沉积和SDD的生成、组成、分布及致病机制均存在差异，研究二者形成机制的差异及交互信息将丰富对AMD发病机制的认识与理解。

利益冲突 所有作者均声明不存在利益冲突。

开放获取声明

本文适用于知识共享许可协议(Creative Commons)，允许第三方用户按照署名(BY)-非商业性使用(NC)-禁止演绎(ND)(CC BY-NC-ND)的方式共享，即允许第三方对本刊发表的文章进行复制、发行、展览、表演、放映、广播或通过信息网络向公众传播，但在这些过程中必须保留作者署名、仅限于非商业性目的、不得进行演绎创作。

参考文献

1. Guymer RH, Campbell TG. Age-related macular degeneration[J]. Lancet, 2023, 401(10386): 1459-1472. DOI:10.1016/s0140-6736(22)02609-5.
2. Curcio CA, Johnson M, Huang JD, et al. Aging, age-related macular degeneration, and the response-to-retention of apolipoprotein B-containing lipoproteins[J]. Prog Retin Eye Res, 2009, 28(6): 393-422. DOI:10.1016/j.preteyeres.2009.08.001.
3. Gariano RF, Gardner TW. Retinal angiogenesis in development and disease[J]. Nature, 2005, 438(7070): 960-966. DOI:10.1038/nature04482.
4. 俞素勤.浅谈“外层视网膜病变”的诊断[J].中华眼底病杂志, 2021, 37(12): 911-914. DOI:10.3760/cma.j.cn511434-20211210-00696 (2021).
   Yu SQ. A brief talk about the diagnosis of "outer retinopathy" — based on the recognition and understanding of optical coherence tomography images. Chin J Ocul Fundus Dis, 2021, 37(12): 911-914. DOI:10.3760/cma.j.cn511434-20211210-00696 (2021).
5. Mrejen S, Sato T, Curcio CA, et al. Assessing the cone photoreceptor mosaic in eyes with pseudodrusen and soft Drusen in vivo using adaptive optics imaging[J]. Ophthalmology, 2014, 121(2): 545-551. DOI:10.1016/j.ophtha.2013.09.026.
6. Lakkaraju A, Umapathy A, Tan LX, et al. The cell biology of the retinal pigment epithelium[J]. Prog Retin Eye Res, 2020, 78: 100846. DOI:10.1016/j.preteyeres.2020.100846.
7. Caceres PS, Rodriguez-Boulan E. Retinal pigment epithelium polarity in health and blinding diseases[J]. Curr Opin Cell Biol, 2020, 62: 37-45. DOI:10.1016/j.ceb.2019.08.001.
8. Kaarniranta K, Blasiak J, Liton P, et al. Autophagy in age-related macular degeneration[J]. Autophagy, 2023, 19(2): 388-400. DOI:10.1080/15548627.2022.2069437.
9. Booij JC, Baas DC, Beisekeeva J, et al. The dynamic nature of bruch's membrane[J]. Prog Retin Eye Res, 2010, 29(1): 1-18. DOI:10.1016/j.preteyeres.2009.08.003.
10. Zhang Y, Huang J, Liang Y, et al. Clearance of lipid droplets by chimeric autophagy-tethering compound ameliorates the age-related macular degeneration phenotype in mice lacking APOE[J]. Autophagy, 2023, 19(10): 2668-2681. DOI:10.1080/15548627.2023.2220540.
11. Yako T, Otsu W, Nakamura S, et al. Lipid droplet accumulation promotes RPE dysfunction[J]. Int J Mol Sci, 2022, 23(3): 1790. DOI:10.3390/ijms23031790.
12. Fleckenstein M, Keenan TDL, Guymer RH, et al. Age-related macular degeneration[J]. Nat Rev Dis Primers, 2021, 7: 31. DOI:10.1038/s41572-021-00265-2.
13. Chen L, Messinger JD, Sloan KR, et al. Nonexudative macular neovascularization supporting outer retina in age-related macular degeneration: a clinicopathologic correlation[J]. Ophthalmology, 2020, 127(7): 931-947. DOI:10.1016/j.ophtha.2020.01.040.
14. Chen L, Messinger JD, Kar D, et al. Biometrics, impact, and significance of basal linear deposit and subretinal drusenoid deposit in age-related macular degeneration[J]. Invest Ophthalmol Vis Sci, 2021, 62(1): 33. DOI:10.1167/iovs.62.1.33.
15. Curcio CA, Brett Presley J, Malek G, et al. Esterified and unesterified cholesterol in drusen and basal deposits of eyes with age-related maculopathy[J]. Exp Eye Res, 2005, 81(6): 731-741. DOI:10.1016/j.exer.2005.04.012.
16. Song D, Mohammed I, Bhuyan R, et al. Retinal basal laminar deposits in complement fH/fP mouse model of dense deposit disease[J]. Invest Ophthalmol Vis Sci, 2018, 59(8): 3405-3415. DOI:10.1167/iovs.18-24133.
17. van der Schaft TL, Mooy CM, de Bruijn WC, et al. Histologic features

of the early stages of age-related macular degeneration. A statistical analysis[J]. Ophthalmology, 1992, 99(2): 278-286. DOI:10.1016/s0161-6420(92)31982-7.

18. Curcio CA. Soft drusen in age-related macular degeneration: biology and targeting via the oil spill strategies[J]. Invest Ophthalmol Vis Sci, 2018, 59(4): AMD160-AMD181. DOI:10.1167/iovs.18-24882.
19. Espinosa-Heidmann DG, Suner IJ, Catanuto P, et al. Cigarette smoke-related oxidants and the development of sub-RPE deposits in an experimental animal model of dry AMD[J]. Invest Ophthalmol Vis Sci, 2006, 47(2): 729-737. DOI:10.1167/iovs.05-0719.
20. Dithmar S, Sharara NA, Curcio CA, et al. Murine high-fat diet and laser photochemical model of basal deposits in Bruch membrane[J]. Arch Ophthalmol, 2001, 119(11): 1643-1649. DOI:10.1001/archopht.119.11.1643.
21. Milam AH, Curcio CA, Cideciyan AV, et al. Dominant late-onset retinal degeneration with regional variation of sub-retinal pigment epithelium deposits, retinal function, and photoreceptor degeneration[J]. Ophthalmology, 2000, 107(12): 2256-2266. DOI:10.1016/s0161-6420(00)00419-x.
22. Weber BH, Vogt G, Pruett RC, et al. Mutations in the tissue inhibitor of metalloproteinases-3 (TIMP3) in patients with Sorsby's fundus dystrophy[J]. Nat Genet, 1994, 8(4): 352-356. DOI:10.1038/ng1294-352.
23. Sura AA, Chen L, Messinger JD, et al. Measuring the contributions of basal laminar deposit and bruch's membrane in age-related macular degeneration[J]. Invest Ophthalmol Vis Sci, 2020, 61(13): 19. DOI:10.1167/iovs.61.13.19.
24. Sura AA, Chen L, Messinger JD, et al. Measuring the contributions of basal laminar deposit and bruch's membrane in age-related macular degeneration[J]. Invest Ophthalmol Vis Sci, 2020, 61(13): 19. DOI:10.1167/iovs.61.13.19.
25. van der Schaft TL, de Bruijnz WC, Mooy CM, et al. Basal laminar deposit in the aging peripheral human retina[J]. Graefe's Arch Clin Exp Ophthalmol, 1993, 231(8): 470-475. DOI:10.1007/bf02044234.
26. Gehrs KM, Anderson DH, Johnson LV, et al. Age-related macular degeneration: emerging pathogenetic and therapeutic concepts[J]. Ann Med, 2006, 38(7): 450-471. DOI:10.1080/07853890600946724.
27. Chen S, Abu-Qamar O, Kar D, et al. Ultrahigh resolution OCT markers of normal aging and early age-related macular degeneration[J]. Ophthalmol Sci, 2023, 3(3): 100277. DOI:10.1016/j.xops.2023.100277.
28. Pilgrim MG, Lengyel I, Lanzirotti A, et al. Subretinal pigment epithelial deposition of drusen components including hydroxyapatite in a primary cell culture model[J]. Invest Ophthalmol Vis Sci, 2017, 58(2): 708-719. DOI:10.1167/iovs.16-21060.
29. Sarks S, Cherepanoff S, Killingsworth M, et al. Relationship of Basal laminar deposit and membranous debris to the clinical presentation of early age-related macular degeneration[J]. Invest Ophthalmol Vis Sci, 2007, 48(3): 968-977. DOI:10.1167/iovs.06-0443.
30. Curcio CA, Millican CL. Basal linear deposit and large drusen are specific for early age-related maculopathy[J]. Arch Ophthalmol, 1999, 117(3): 329-339. DOI:10.1001/archopht.117.3.329.
31. Ruberti JW, Curcio CA, Millican CL, et al. Quick-freeze/deep-etch visualization of age-related lipid accumulation in Bruch's membrane[J]. Invest Ophthalmol Vis Sci, 2003, 44(4): 1753-1759. DOI:10.1167/iovs.02-0496.
32. Johnson M, Dabholkar A, Huang JD, et al. Comparison of morphology of human macular and peripheral Bruch's membrane in older eyes[J]. Curr Eye Res, 2007, 32(9): 791-799. DOI:10.1080/02713680701550660.
33. Curcio CA, Johnson M, Rudolf M, et al. The oil spill in ageing Bruch membrane[J]. Br J Ophthalmol, 2011, 95(12): 1638-1645. DOI:10.1136/bjophthalmol-2011-300344.
34. Yang YC, Chien Y, Yarmishyn AA, et al. Inhibition of oxidative stress-induced epithelial-mesenchymal transition in retinal pigment epithelial cells of age-related macular degeneration model by suppressing ERK activation[J]. J Adv Res, 2024, 60: 141-157. DOI:10.1016/j.jare.2023.06.004.
35. Kaarniranta K, Uusitalo H, Blasiak J, et al. Mechanisms of mitochondrial dysfunction and their impact on age-related macular degeneration[J]. Prog Retin Eye Res, 2020, 79: 100858. DOI:10.1016/j.preteyeres.2020.100858.
36. Toomey CB, Johnson LV, Bowes Rickman C. Complement factor H in AMD: bridging genetic associations and pathobiology[J]. Prog Retin Eye Res, 2018, 62: 38-57. DOI:10.1016/j.preteyeres.2017.09.001.
37. Pikuleva IA, Curcio CA. Cholesterol in the retina: the best is yet to come[J]. Prog Retin Eye Res, 2014, 41: 64-89. DOI:10.1016/j.preteyeres.2014.03.002.
38. Curcio CA, Johnson M. Cholesteryl ester transfer protein inhibitors and access to the retina in age-related macular degeneration[J]. JAMA Cardiol, 2023, 8(2): 206. DOI:10.1001/jamacardio.2022.4808.
39. El-Darzi N, Mast N, Li Y, et al. APOB100 transgenic mice exemplify how the systemic circulation content may affect the retina without altering retinal cholesterol input[J]. Cell Mol Life Sci, 2024, 81(1): 52. DOI:10.1007/s00018-023-05056-4.
40. Jun S, Datta S, Wang L, et al. The impact of lipids, lipid oxidation, and inflammation on AMD, and the potential role of miRNAs on lipid metabolism in the RPE[J]. Exp Eye Res, 2019, 181: 346-355.

DOI:10.1016/j.exer.2018.09.023.

41. Souied EH, Benlian P, Amouyel P, et al. The epsilon4 allele of the apolipoprotein E gene as a potential protective factor for exudative age-related macular degeneration[J]. Am J Ophthalmol, 1998, 125(3): 353-359. DOI:10.1016/s0002-9394(99)80146-9.
42. Neale BM, Fagerness J, Reynolds R, et al. Genome-wide association study of advanced age-related macular degeneration identifies a role of the hepatic lipase gene (LIPC)[J]. Proc Natl Acad Sci USA, 2010, 107(16): 7395-7400. DOI:10.1073/pnas.0912019107.
43. Chen W, Stambolian D, Edwards AO, et al. Genetic variants near TIMP3 and high-density lipoprotein-associated loci influence susceptibility to age-related macular degeneration[J]. Proc Natl Acad Sci USA, 2010, 107(16): 7401-7406. DOI:10.1073/pnas.0912702107.
44. Huang JD, Brett Presley J, Chimento MF, et al. Age-related changes in human macular Bruch's membrane as seen by quick-freeze/deep-etch[J]. Exp Eye Res, 2007, 85(2): 202-218. DOI:10.1016/j.exer.2007.03.011.
45. Curcio CA, Brett Presley J, Leigh Millican C, et al. Basal deposits and drusen in eyes with age-related maculopathy: evidence for solid lipid particles[J]. Exp Eye Res, 2005, 80(6): 761-775. DOI:10.1016/j.exer.2004.09.017.
46. Chen L, Yang P, Curcio CA. Visualizing lipid behind the retina in aging and age-related macular degeneration, via indocyanine green angiography (ASHS-LIA)[J]. Eye (Lond), 2022, 36(9): 1735-1746. DOI:10.1038/s41433-022-02016-3.
47. Chen L, Zhang X, Liu B, et al. Age-related scattered hypofluorescent spots on late-phase indocyanine green angiography: the multimodal imaging and relevant factors[J]. Clin Exp Ophthalmol, 2018, 46(8): 908-915. DOI:10.1111/ceo.13306.
48. Chen L, Zhang X, Li M, et al. Drusen and age-related scattered hypofluorescent spots on late-phase indocyanine green angiography, a candidate correlate of lipid accumulation[J]. Invest Ophthalmol Vis Sci, 2018, 59(12): 5237-5245. DOI:10.1167/iovs.18-25124.
49. Chen L, Messinger JD, Sloan KR, et al. Abundance and multimodal visibility of soft drusen in early age-related macular degeneration: a Clinicopathologic Correlation[J]. Retina, 2020, 40(8): 1644-1648. DOI:10.1097/iae.0000000000002893.
50. Li M, Dolz-Marco R, Messinger JD, et al. Clinicopathologic correlation of aneurysmal type 1 neovascularization in age-related macular degeneration[J]. Ophthalmol Retina, 2019, 3(2): 99-111. DOI:10.1016/j.oret.2018.08.008.
51. Chen L, Zhang X, Li M, et al. Age-related scattered hypofluorescent spots on late-phase indocyanine green angiography as precursor lesions of polypoidal choroidal vasculopathy[J]. Invest Ophthalmol Vis Sci, 2019, 60(6): 2102-2109. DOI:10.1167/iovs.19-26968.
52. Mori F, Eguchi S. Polypoidal choroidal vasculopathy[J]. Br J Ophthalmol, 2007, 91(9): 1104-1105. DOI:10.1136/bjo.2007.116178.
53. Curcio CA. Antecedents of soft drusen, the specific deposits of age-related macular degeneration, in the biology of human macula[J]. Invest Ophthalmol Vis Sci, 2018, 59(4): AMD182-AMD194. DOI:10.1167/iovs.18-24883.
54. Ferris FL 3rd, Wilkinson CP, Bird A, et al. Clinical classification of age-related macular degeneration[J]. Ophthalmology, 2013, 120(4): 844-851. DOI:10.1016/j.ophtha.2012.10.036.
55. Krytkowska E, Grabowicz A, Safranow K, et al. Does the presence of the cilioretinal artery affect the incidence, clinical picture and progression of age-related macular degeneration?[J]. Diagnostics, 2023, 13(9): 1593. DOI:10.3390/diagnostics13091593.
56. Chen L, Messinger JD, Ferrara D, et al. Stages of drusen-associated atrophy in age-related macular degeneration visible via histologically validated fundus autofluorescence[J]. Ophthalmol Retina, 2021, 5(8): 730-742. DOI:10.1016/j.oret.2020.11.006.
57. Tran TM, Kim S, Lin KH, et al. Quantitative fundus autofluorescence in rhesus macaques in aging and age-related drusen[J]. Invest Ophthalmol Vis Sci, 2020, 61(8): 16. DOI:10.1167/iovs.61.8.16.
58. Yiu G, Chung SH, Mollhoff IN, et al. Long-term evolution and remodeling of soft drusen in rhesus macaques[J]. Invest Ophthalmol Vis Sci, 2020, 61(2): 32. DOI:10.1167/iovs.61.2.32.
59. Schaal KB, Rosenfeld PJ, Gregori G, et al. Anatomic clinical trial endpoints for nonexudative age-related macular degeneration[J]. Ophthalmology, 2016, 123(5): 1060-1079. DOI:10.1016/j.ophtha.2016.01.034.
60. Bressler NM, Munoz B, Maguire MG, et al. Five-year incidence and disappearance of drusen and retinal pigment epithelial abnormalities. Waterman study[J]. Arch Ophthalmol, 1995, 113(3): 301-308. DOI:10.1001/archopht.1995.01100030055022.
61. Sarks JP, Sarks SH, Killingsworth MC. Evolution of geographic atrophy of the retinal pigment epithelium[J]. Eye, 1988, 2 (Pt 5): 552-577. DOI:10.1038/eye.1988.106.
62. Cukras C, Agrón E, Klein ML, et al. Natural history of drusenoid pigment epithelial detachment in age-related macular degeneration: Age-Related Eye Disease Study Report No. 28[J]. Ophthalmology, 2010, 117(3): 489-499. DOI:10.1016/j.ophtha.2009.12.002.
63. Rudolf M, Clark ME, Chimento MF, et al. Prevalence and morphology of Druse types in the macula and periphery of eyes with age-related maculopathy[J]. Invest Ophthalmol Vis Sci, 2008, 49(3): 1200-1209. DOI:10.1167/iovs.07-1466.
64. Ding X, Patel M, Chan CC. Molecular pathology of age-related macular

degeneration[J]. Prog Retin Eye Res, 2009, 28(1): 1-18. DOI:10.1016/j.preteyeres.2008.10.001.

65. Pedersen HR, Gilson SJ, Dubra A, et al. Multimodal imaging of small hard retinal drusen in young healthy adults[J]. Br J Ophthalmol, 2018, 102(1): 146-152. DOI:10.1136/bjophthalmol-2017-310719.
66. Munch IC, Sander B, Kessel L, et al. Heredity of small hard drusen in twins aged 20–46 years[J]. Invest Ophthalmol Vis Sci, 2007, 48(2): 833. DOI:10.1167/iovs.06-0529.
67. Munch IC, Li XQ, Ahmad SSM, et al. Small hard macular drusen and associations in 11- to 12-year-old children in the Copenhagen child cohort 2000 eye study[J]. Invest Ophthalmol Vis Sci, 2019, 60(5): 1454-1460. DOI:10.1167/iovs.18-25877.
68. Balaratnasingam C, Cherepanoff S, Dolz-Marco R, et al. Cuticular drusen: clinical phenotypes and natural history defined using multimodal imaging[J]. Ophthalmology, 2018, 125(1): 100-118. DOI:10.1016/j.ophtha.2017.08.033.
69. Yoon JM, Shin DH, Kong M, et al. Age-related macular degeneration eyes presenting with cuticular drusen and reticular pseudodrusen[J]. Sci Rep, 2022, 12(1): 5681. DOI:10.1038/s41598-022-09608-9.
70. Boon CJF, van de Ven JPH, Hoyng CB, et al. Cuticular drusen: stars in the sky[J]. Prog Retin Eye Res, 2013, 37: 90-113. DOI:10.1016/j.preteyeres.2013.08.003.
71. Evers CD, Chen L, Messinger JD, et al. Histology, dimensions, and fluorescein staining characteristics of nodular and cuticular drusen in age-related macular degeneration[J]. Retina, 2023, 43(10): 1708-1716. DOI:10.1097/iae.0000000000003871.
72. Goh KL, Chen FK, Balaratnasingam C, et al. Cuticular drusen in age-related macular degeneration: association with progression and impact on visual sensitivity[J]. Ophthalmology, 2022, 129(6): 653-660. DOI:10.1016/j.ophtha.2022.01.028.
73. Charng J, Balaratnasingam C, Attia MS, et al. Localised relative scotoma in cuticular drusen[J]. Graefes Arch Clin Exp Ophthalmol, 2022, 260(7): 2157-2164. DOI:10.1007/s00417-022-05570-4.
74. Nam SW, Lee JH, Byun Z, et al. Evaluation of the microperimetry in eyes with cuticular drusen[J]. Sci Rep, 2022, 12(1): 17557. DOI:10.1038/s41598-022-22513-5.
75. Spaide RF, Ooto S, Curcio CA. Subretinal drusenoid deposits AKA pseudodrusen[J]. Surv Ophthalmol, 2018, 63(6): 782-815. DOI:10.1016/j.survophthal.2018.05.005.
76. Oak ASW, Messinger JD, Curcio CA. Subretinal drusenoid deposits: further characterization by lipid histochemistry[J]. Retina, 2014, 34(4): 825-826. DOI:10.1097/IAE.0000000000000121.
77. Digsby K, Zhang Q, Miller JML. Basic science observations link subretinal drusenoid deposit formation to retinal pigment epithelial hypoxia[J]. Eye, 2024. DOI:10.1038/s41433-024-03167-1.
78. Wu Z, Fletcher EL, Kumar H, et al. Reticular pseudodrusen: a critical phenotype in age-related macular degeneration[J]. Prog Retin Eye Res, 2022, 88: 101017. DOI:10.1016/j.preteyeres.2021.101017.
79. Chen L, Messinger JD, Zhang Y, et al. Subretinal drusenoid deposit in age-related macular degeneration: Histologic Insights Into Initiation, Progression to Atrophy, and Imaging[J]. Retina, 2020, 40(4): 618-631. DOI:10.1097/IAE.0000000000002657.
80. Querques G, Srour M, Massamba N, et al. Reticular pseudodrusen[J]. Ophthalmology, 2013, 120(4): 872-872.e4. DOI:10.1016/j.ophtha.2012.12.007.
81. De Bats F, Mathis T, Mauget-Faÿsse M, et al. Prevalence of reticular pseudodrusen in age-related macular degeneration using multimodal imaging[J]. Retina, 2016, 36(1): 46-52. DOI:10.1097/IAE.0000000000000648.
82. Querques G, Canouï-Poitrine F, Coscas F, et al. Analysis of progression of reticular pseudodrusen by spectral domain-optical coherence tomography[J]. Invest Ophthalmol Vis Sci, 2012, 53(3): 1264-1270. DOI:10.1167/iovs.11-9063.
83. Menean M, Sacconi R, Tombolini B, et al. Reticular pseudodrusen disappearance after development of macular neovascularization[J]. Retina, 2024, 44(10): 1688-1695. DOI:10.1097/iae.0000000000004173.
84. Huang BB, Fawzi AA. Disentangling the impact of reticular pseudodrusen phenotype and the ARMS2/HTRA1 risk allele in geographic atrophy: the AREDS 2 study report 32[J]. Ophthalmology, 2023, 130(5): 460-461. DOI:10.1016/j.ophtha.2023.02.010.
85. Domalpally A, Agrón E, Pak JW, et al. Prevalence, risk, and genetic association of reticular pseudodrusen in age-related macular degeneration: age-related eye disease study 2 report 21[J]. Ophthalmology, 2019, 126(12): 1659-1666. DOI:10.1016/j.ophtha.2019.07.022.
86. Cohen SY, Dubois L, Tadayoni R, et al. Prevalence of reticular pseudodrusen in age-related macular degeneration with newly diagnosed choroidal neovascularisation[J]. Br J Ophthalmol, 2007, 91(3): 354-359. DOI:10.1136/bjo.2006.101022.

(**责任编委**：朱艳吉；**编辑**：殷秋霞)